Electronic Supplementary Material

Building in Biologically Appropriate Multifunctionality in Aqueous Copper Indium Selenide Based Quantum Dots

Xiling Yang[a], Yun Li[a], Peisen Zhang[b,c,*], Lingfei Guo[a], Xiaoqi Li[a], Yiyang Shu[a], Kuiyu Jiang[a], Yi Hou[c], Lihong Jing[b,*], Mingxia Jiao[a,*]

[a] *Key Laboratory of Optic-electric Sensing and Analytical Chemistry for Life Science, MOE, College of Chemistry and Molecular Engineering, Qingdao University of Science and Technology, Zhengzhou Road 53, Qingdao 266042, China*

[b] *Key Laboratory of Colloid, Interface and Chemical Thermodynamics, Institute of Chemistry, Chinese Academy of Sciences Bei Yi Jie 2, Zhong Guan Cun, Beijing 100190, China*

[c] *College of Life Science and Technology, Beijing University of Chemical Technology, Beijing, 10029, China.*

Address correspondence to zhangps@iccas.ac.cn, jinglh@iccas.ac.cn, jiaomingxia@qust.edu.cn

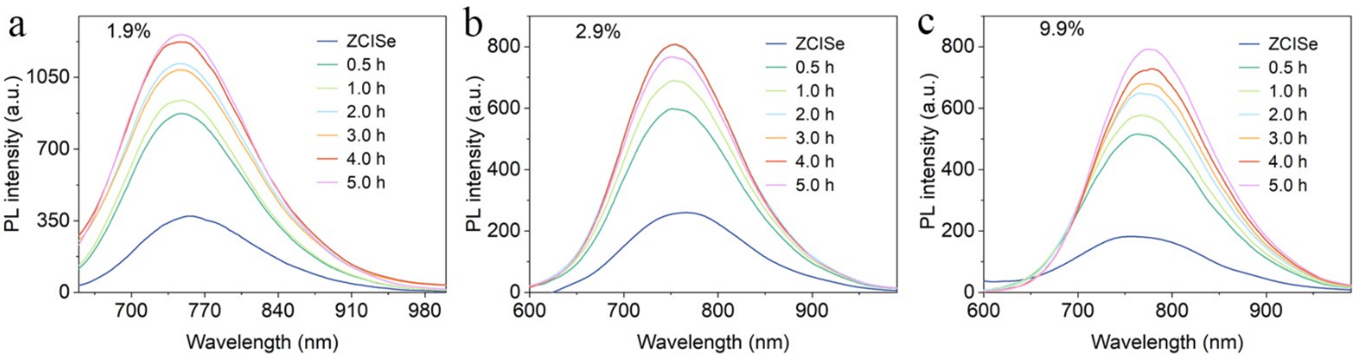

Fig. S1 Temporal evolutions of PL spectra of Zn-Cu-In-Se@ZnS:Mn QDs with different Mn doping levels.

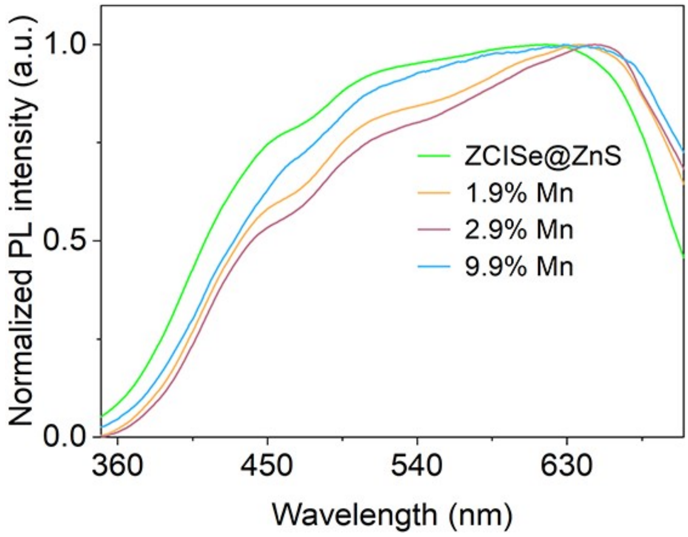

Fig. S2 Excitation spectra of Zn-Cu-In-Se@ZnS QDs and Zn-Cu-In-Se@ZnS:Mn QDs with different Mn doping levels.

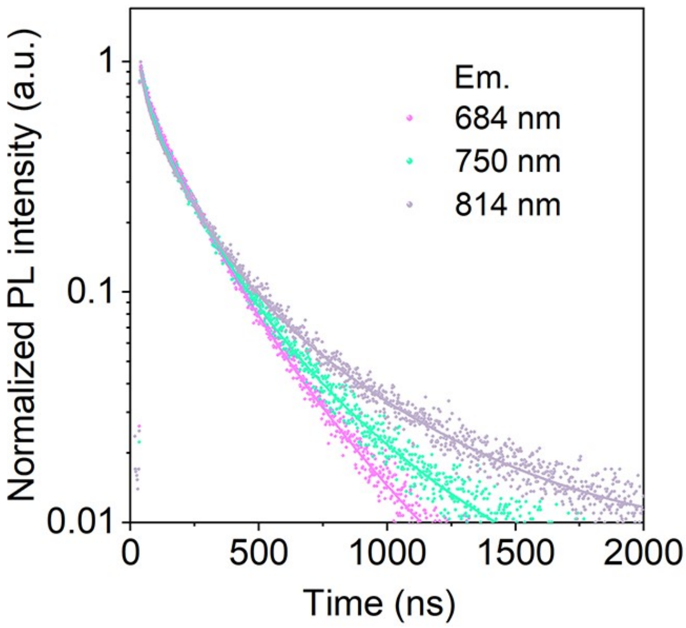

Fig. S3 Time-resolved PL decay curves of Zn-Cu-In-Se@ZnS QDs at different emission wavelengths.

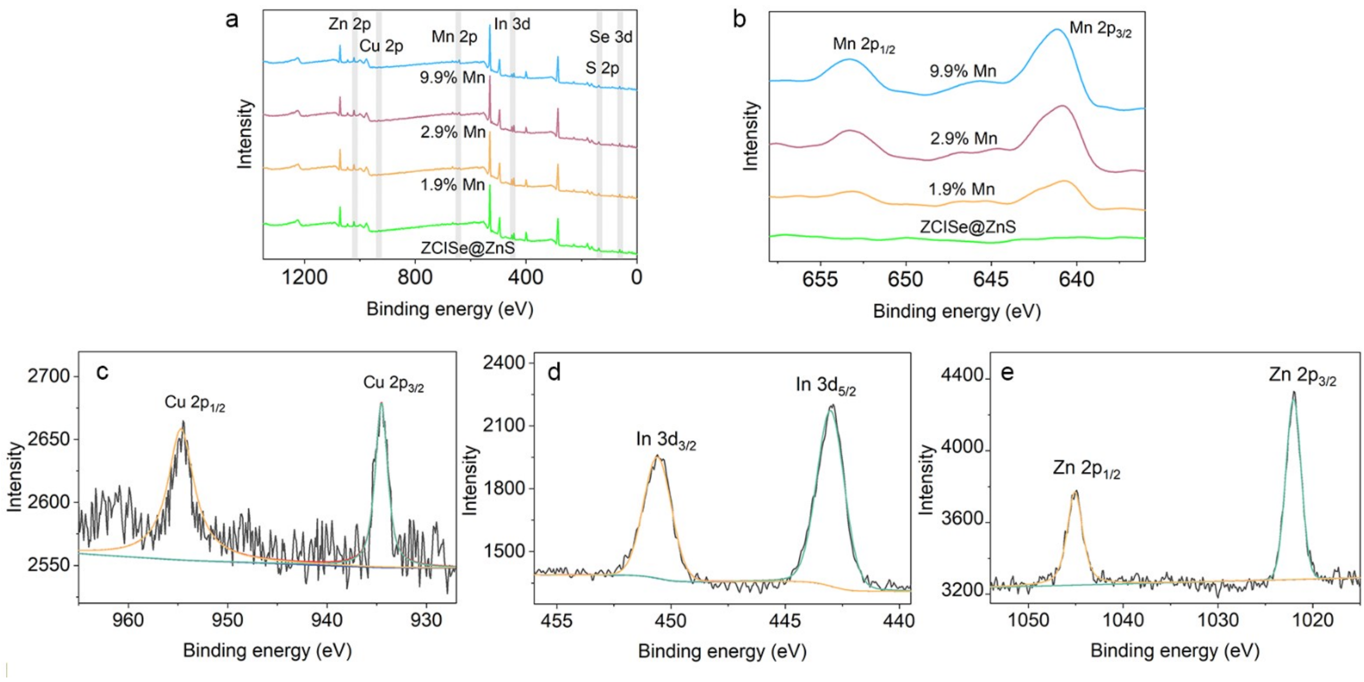

Fig. S4 XPS spectra of Zn-Cu-In-Se@ZnS QDs and Zn-Cu-In-Se@ZnS:Mn QDs with different Mn doping levels (a) together with the amplified spectra for Mn element (b), and high-resolution XPS signals of Cu 2p (c), In 3d (d), and Zn 2p (e) including the experimental results and the fitting results for the QDs with a Mn doping level of 9.9%.

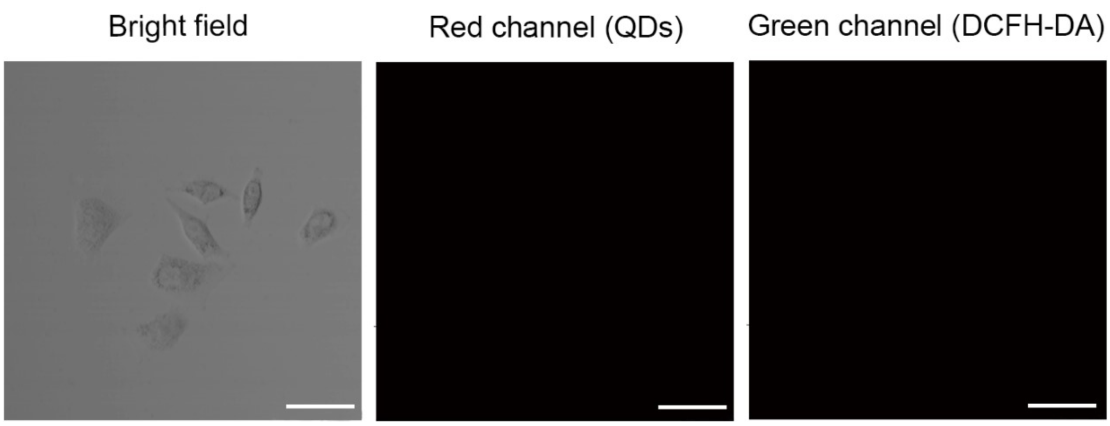

Fig. S5 Bright field and confocal fluorescence images of MCF-7 cells treated with 1× PBS, and the scale bars correspond to 75 μm.

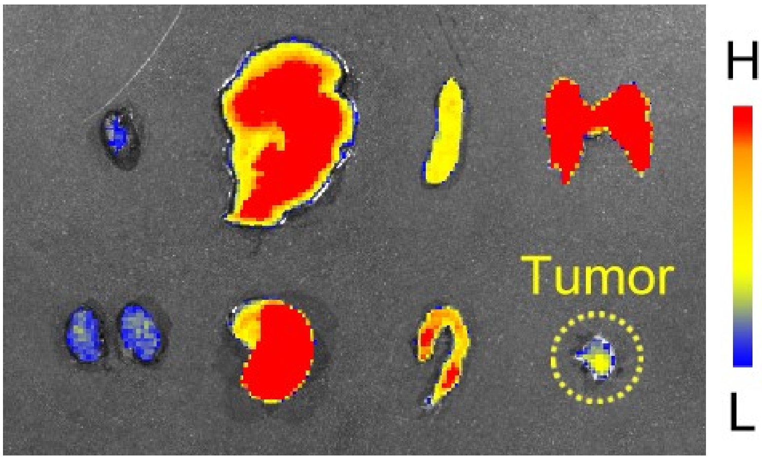

Fig. S6 Ex vivo $\lambda_{ex}605/\lambda_{em}780$ channel fluorescence image of the major organs including heart, liver, spleen, lung, and kidney, as well as the tumor tissue captured at 4 h after injection of QDs.

Time-resolved photoluminescence (TR PL) measurements

The PL decay curves were fit using the multi-exponential function:

$$I(t) = \sum_{i=1}^{n} B_i exp(-t/\tau_i), \qquad \sum_{i=1}^{n} B_i = 1 \qquad S(1)$$

In this expression, τ_i represents the decay time constants, B_i represents the normalized amplitudes of each component, and *n* is the number of decay times. Because the photoluminescence decays for all the QDs are best fit using a three-exponential function ($n = 3$), the amplitude-weighted average decay lifetime τ_{avg} of the entire fluorescence decay process was calculated in the form:

$$\tau_{avg} = \frac{\sum B_i \tau_i^2}{\sum B_i \tau_i} \qquad S(2)$$

The normalized lifetime-amplitude product is given as:

$$f_i = \frac{\tau_i B_i}{\sum \tau_i B_i} \qquad S(3)$$

In this expression, f_i represents the relative time-integrated contribution of each respective process to the overall number of emitted photons (i.e., the emission intensity measured in steady state PL spectra).

The radiative and nonradiative recombination rates with the PLQY were further correlated to understand the fluorescence behavior of the QDs with different Mn doping levels. The radiative recombination rate (τ_r^{-1}) can be determined by the experimentally determined PLQY in **Figure 1b** and the measure average PL lifetime (τ_{avg}) in **Table S3** as follows:

$$\tau_r^{-1} = QY \times \tau_{avg}^{-1} \qquad S(4)$$

and then the non-radiative recombination rate (τ_{nr}^{-1}) was calculated assuming no dark fraction of emitters and is given as:

$$\tau_{nr}^{-1} = \tau_{avg}^{-1} - \tau_r^{-1} \qquad S(5)$$

The PL decay-fitting data for all curves are summarized in **Table S3-S5**.

Table S1 The elemental composition of Zn-Cu-In-Se@ZnS:Mn QDs with different Mn doping levels.

Feed proportion of Mn^{2+} (mol %)	Zn:Cu:In:Mn	Mn-doping Level
0 (ZCISe@ZnS)	1.00 : 0.52 : 1.54 : 0	0
12	1.00 : 0.53 : 1.51 : 0.06	1.9%
21	1.00 : 0.45 : 1.27 : 0.08	2.9%
39	1.00 : 0.45 : 1.24 : 0.30	9.9%

Table S2 A comparison of the optical properties of NIR-emitting Cd-free QDs *via* aqueous synthesis.

Types of QDs	Emission maxima [nm]	PLQY [%]	Reference
Ag_2S	1050	2.3 (against IR-26)	1
Ag_2S	835	4.3 (against ICG)	2
Ag_2S (Ag:S = 1.89:1)	1130	1.8	3
Ag_2S	1060	0.04-0.11 (against IR-26)	4
Ag_2S	1060	1.26-1.32 (against IR-26)	5
Ag_2Te	1060	2.1	6
Ag_2Te/ZnS	1070	5.6	
Ag, Mn co-doped In_2S_3/ZnS	743	2.0 (against R6G)	7
$Ag_{0.53}InS_2$	710	36.0	8
$Ag_{1.1}InS_{2.1}$	760	8.0	
$Ag_{0.34}Zn_{0.59}InS_2/(ZnS)_{1.69}$	696	55.0	
Ag-In-S (Ag:In = 1:5.98)	664	4.0	9
$AgInS_2$	720	6.0	10
$AgInZn_2S_4$	660	15.0	
$AgInS_2$	720	8.8	11
Ag-In-S/ZnS (Ag:In = 1:5)	652	0.6	12
Ag-In-S/ZnS (Ag:In = 1:3.3)	716	0.3	
Ag-In-Se/ZnSe (Ag:In = 10:1)	940	7.0	13
Ag-In-Se/ZnS (Ag:In = 1:1.12)	650	20.5	14
Cu-In-S/ZnS (Cu:In = 0.33:1)	746	13.8	15
Cu-In-S (Cu:Zn = 1:2.35)	777	4.4	16
Cu-In-Zn-S (Cu:In:Zn = 1:1.79:5.86)	680	15.7	
Cu-In-Se (Cu:In = 1:5.13)	650	10.3	17
Cu-In-Se/ZnS (Cu:In = 1:3)	824	4.3	18
Cu-In-Se (Cu:In = 1:4.5)	765	1.9	19
Zn-Cu-In-Se@ZnS (Zn:Cu:In = 1:0.52:1.54)	749	25.2	This work
Zn-Cu-In-Se@ZnS:Mn (Zn:Cu In = 1:0.45:1.24, Mn doping ratio of 9.9%)	778	18.9	

Table S3 The parameters for three-exponential fitting of the PL decay curves in **Figure 1d** (i.e., normalized amplitude B_i, time constant τ_i and their normalized products f_i, goodness-of-fit parameter χ^2), together with the emission peak wavelengths of Zn-Cu-In-Se@ZnS:Mn QDs with different Mn doping levels.

Mn/[%]	λ_{em} [nm]	B_1 [%]	f_1 [%]	τ_1 [ns]	B_2 [%]	f_2 [%]	τ_2 [ns]	B_3 [%]	f_3 [%]	τ_3 [ns]	τ_{avg} [ns]	χ^2
0	749	30.9	5.4	29.1	50.7	43.4	150.0	18.4	51.5	490.1	318.8	1.0
1.9%	751	25.8	3.4	27.7	53.5	47.0	152.8	20.7	48.9	409.6	273.1	0.9
2.9%	753	26.5	7.1	20.2	48.5	37.4	121.5	25.0	59.2	372.7	267.0	1.1
9.9%	778	25.7	4.3	27.7	55.2	49.6	147.7	19.2	46.0	394.2	256.0	1.0

Table S4 The parameters for three-exponential fitting of the PL decay curves in **Figure 1f** (i.e., normalized amplitude B_i, time constant τ_i and their normalized products f_i, goodness-of-fit parameter χ^2), for different emission wavelengths of the Zn-Cu-In-Se@ZnS:Mn QDs with the Mn doping level of 9.9%.

λ_{em} [nm]	B_1 [%]	f_1 [%]	τ_1 [ns]	B_2 [%]	f_2 [%]	τ_2 [ns]	B_3 [%]	f_3 [%]	τ_3 [ns]	τ_{avg} [ns]	χ^2
713	22.2	4.3	31.6	55.9	50.3	147.7	21.9	45.4	339.8	230.0	1.1
778	25.7	4.3	27.7	55.2	49.6	147.7	19.2	46.0	394.2	256.0	1.0
842	27.7	4.5	26.3	50.5	42.6	143.7	21.7	53.2	417.4	284.1	1.0

Table S5 The parameters for three-exponential fitting of the PL decay curves in **Figure S3** (i.e., normalized amplitude B_i, time constant τ_i and their normalized products f_i, goodness-of-fit parameter χ^2), for different emission wavelengths of the Zn-Cu-In-Se@ZnS QDs.

λ_{em} [nm]	B_1 [%]	f_1 [%]	τ_1 [ns]	B_2 [%]	f_2 [%]	τ_2 [ns]	B_3 [%]	f_3 [%]	τ_3 [ns]	τ_{avg} [ns]	χ^2

684	37.2	5.9	23.6	45.7	42.7	138.3	17.0	51.4	447.3	290.3	1.0
750	30.9	5.4	29.1	50.7	43.4	150.0	18.4	51.5	490.1	318.8	1.0
814	28.7	5.3	33.6	52.4	45.8	167.1	18.9	49.2	499.2	341.4	1.1

References

1 F. Lu, W. Ju, N. Zhao, T. Zhao, C. Zhan, Q. Wang, Q. Fan, W. Huang, *Biochem. Biophys. Res. Commun.*, 2020, **529**, 930-935.

2 P. Jiang, Z. Chen, *New J. Chem.*, 2017, **41**, 5707-5712.

3 H. Y. Yang, Y. W. Zhao, Z. Y. Zhang, H. M. Xiong, S. N. Yu, *Nanotechnol.*, 2013, **24**, 055706.

4 S. Qu, Q. Jia, Z. Li, Z. Wang, L. Shang, *Sci. Bull.*, 2022, **67**, 1274-1283.

5 T. Yang, Y.a. Tang, L. Liu, X. Lv, Q. Wang, H. Ke, Y. Deng, H. Yang, X. Yang, G. Liu, Y. Zhao, H. Chen, *ACS Nano*, 2017, **11**, 1848-1857.

6 C. Chen, X. He, L. Gao, N. Ma, *ACS Appl. Mater. Interfaces,* 2013, **5**, 1149-1155.

7 P. Y. Lai, C. C. Huang, T. H. Chou, K. L. Ou, J. Y. Chang, *Acta. Biomater.*, 2017, **50**, 522-533.

8 A. Delices, D. Moodelly, C. Hurot, Y. Hou, W. L. Ling, C. Saint-Pierre, D. Gasparutto, G. Nogues, P. Reiss, K. Kheng, *ACS Appl. Mater. Interfaces*, 2020, **12**, 44026-44038.

9 L. Fu, K. Fu, X. Gao, S. Dong, B. Zhang, S. Fu, H. Y. Hu, G. Zou, *Anal. Chem.*, 2021, **93**, 2160-2165.

10 N. Gao, R. Zhang, B. Chen, J. Zhang, X. Zhang, A.L. Rogach, *Nano Res.*, 2020, **14**, 2321-2329.

11 J. Wang, H. T. Ma, L. J. Pan, L. Zhang, Z. L. Zhang, *Chinese Chem. Lett.*, 2022, **33**, 3767-3771.

12 I. V. Martynenko, A. S. Baimuratov, F. Weigert, J. X. Soares, L. Dhamo, P. Nickl, I. Doerfel, J. Pauli, I. D. Rukhlenko, A.V. Baranov, U. Resch-Genger, *Nano Res.*, 2019, **12**, 1595-1603.

13 D. Che, X. Zhu, H. Wang, Y. Duan, Q. Zhang, Y. Li, *J. Colloid Interf. Sci*, 2016, **463**, 1-7.

14 X. Kang, Y. Yang, L. Huang, Y. Tao, L. Wang, D. Pan, *Green Chem.*, 2015, **17**, 4482-4488.

15 M. Jiao, X. Huang, L. Ma, Y. Li, P. Zhang, X. Wei, L. Jing, X. Luo, A.L. Rogach, M. Gao, *Chem. Commun.*, 2019, **55**, 15053-15056.

16 X. Y. Liu, G. Zhang, H. Chen, H. Li, J. Jiang, Y. T. Long, Z. Ning, *Nano Res.*, 2018, **11**, 1379-1388..

17 J. Chen, L. Zhang, S. Li, F. L. Jiang, P. Jiang, Y. Liu, *ACS Applied Nano Materials*, 2021, **4**, 6057-6066.

18 Y. Jia, H. Liu, P. Cai, X. Liu, L. Wang, L. Ding, G. Xu, W. Wang, M. Jiao, X. Luo, *Chem. Commun.*, 2021, **57**, 4178-4181.

19 S. Qu, X. Yuan, Y. Li, X. Li, X. Zhou, X. Xue, K. Zhang, J. Xu, C. Yuan, *Nanoscale*, 2021, **3**, 2334-2342.